

A Method for Calculating the Pressure Drop in Honeycomb Dies

S. Blackburn & H. Böhm

IRC in Materials for High Performance Applications and School of Chemical Engineering, The University of Birmingham, Edgbaston, Birmingham B15 2TT, UK

(Received 15 September 1995; accepted 23 July 1996)

Abstract

Three ceramic pastes based on alumina with different binder systems were characterised using physically based equations and the pressure drop measured as they passed through an experimental honeycomb die. Using an additive approach the pressure drop through the honeycomb die was predicted from the paste parameters derived by the characterisation method and the results compared with the experimentally determined pressure losses. In simple pastes based on a clay–starch binder system, where their pressure–velocity relationships were near-linear and the die entry velocity dependence was small, the predicted and experimental values were in reasonable agreement ($\pm 10\%$) but in more complex systems using polymer solution binders the fit was less accurate (-10 to -45%) for the best of the four models evaluated. This was attributed to the divergent flow in the die on passage from the die holes to slots which at present cannot be modelled using the method of analysis adopted. © 1996 Elsevier Science Limited.

Notation

A_h	Open area of holes (m^3)
A_s	Open area of slots (m^3)
D_h	Diameter of holes (m^3)
D_0	Barrel diameter (m)
D_1	Diameter of a circle just touching the outer most holes [D_h] (m)
L_1	Length of holes (m)
L_2	Length of slot (m)
n	Number of holes
P	Total pressure drop in system (Pa)
P_A	Pressure drop into holes (Pa)
P_B	Pressure drop into holes via intermediate equation (Pa)
P_C	Pressure drop through holes (Pa)
P_D	Pressure drop hole-slot transition [A_h/A_s] (Pa)

P_E	Pressure drop hole-slot transition [A_h /modified A_s] (Pa)
P_F	Pressure drop through slots (Pa)
P_1	Pressure drop for convergent flow in round dies, die entry (Pa)
P_2	Pressure drop for parallel flow in round dies, die land (Pa)
Q	Volumetric flow rate (m^3/s)
S_w	Slot width (m)
V	Velocity of the extrudate (m/s)
V_0	Barrel velocity (m/s)
V_1	Velocity of the paste passing D_1 (m/s)
V_2	Velocity of paste in die holes (m/s)
α	Velocity factor of bulk yield stress, bulk velocity factor ($m=1$) ($Pa\ s\ m^{-1}$)
α_1	Velocity factor of bulk yield stress, bulk velocity factor ($m \neq 1$) ($Pa\ [s\ m^{-1}]^m$)
β	Velocity factor of wall shear stress, wall velocity factor ($n=1$) ($Pa\ s\ m^{-1}$)
β_1	Velocity factor of wall shear stress, wall velocity factor ($n \neq 1$) ($Pa\ [s\ m^{-1}]^n$)
σ_0	Bulk yield stress at low viscosity; initial bulk stress (Pa)
τ_0	Initial wall shear stress of paste: initial wall shear stress (Pa)

Introduction

Complex ‘honeycomb’ structures¹ are now routinely extruded for ceramic catalyst supports and other applications. Many millions of support structures are produced for the automotive industry annually. The market is expanding as legislation dictates the use of such devices throughout the world. Honeycomb structured particulate materials are finding applications in other aspects of gas cleaning and structural products. In the basic die design for these structures, the paste enters the die through an array of geometrically placed holes which intercept a network of slots which give the final shape.² A pressure drop is developed as the

paste is forced through the die, the magnitude of which will depend on, for example, the paste, the number of cells per unit area and the wall thickness of the honeycomb. The pressure drop in the dies is of interest to plant operators and designers. Here a simple approach to modelling such dies is considered.

Experimental Procedure

Paste formulation

Three types of pastes were prepared for the characterisation of flow through a model honeycomb die.

Type I

In this paste three α -alumina powders with mean equivalent spherical diameters of 2.9, 10 and 29 μm (measured by Sedigraph X-ray sedimentometry, F1500, F400, F280, Universal Ceramic Materials, UK) and in the ratio 1:1:1 were mixed with a binder containing 15.8 wt% Wyoming bentonite clay, 15.8 wt% starch and 68.4 wt% distilled water.

Type II

A fine calcined alumina, d_{50} 0.50 μm (RA 107 LS, Baco, UK) was mixed with a 4.0 wt% solution of hydroxypropylmethyl-cellulose (HPMC) (Grade B2/15, Courtaulds Chemicals, UK).

Type III

These pastes had the same formulation as Type II with glycerol added at ≈ 0.5 wt% to the binder solution.

Pastes of different rheology were prepared by varying the amount of binder. The level of moisture was determined for each of the eleven pastes produced by taking the average moisture calculated from the weight loss at 110°C in three specimens of approximately 20 g each, Table 1. In all cases the powders were premixed for 5 min in a planetary mixer (Kenwood, UK), then the water was added and mixed for 40 min in a high-shear kneader (LUK 3III-2Vak, Werner and Pfleiderer, D); the mixer was water-cooled to 15°C.

Table 1. Paste formulation (numbers in parentheses refer to paste number)

	Type I	Type II	Type III
Moisture (wt%)	13.39 (1)	18.43 (6)	17.42 (9)
	14.05 (2)	18.98 (7)	17.90 (10)
	14.06 (3)	19.54 (8)	18.36 (11)
	14.72 (4)		
	15.46 (5)		

Paste characterisation

The pressure drop, P , in pastes during extrusion through circular dies can be characterised using equations proposed by Benbow *et al.*³ of the general form

$$P = P_1 + P_2 = 2(\sigma_0 + \alpha_1 V^m) \ln \left(\frac{D_0}{D} \right) + 4(\tau_0 + \beta_1 V^n) \left(\frac{L}{D} \right) \quad (1)$$

where P_1 and P_2 are the die entry and die land pressure drops, respectively, D_0 is the barrel diameter, D is the die diameter, L is the die land length and V is the velocity of the extrudate. The six paste parameters which characterise the pastes' rheology are: σ_0 , the bulk yield stress of the paste, α_1 , the velocity factor of the bulk yield stress when $m \neq 1$, m , the bulk velocity exponent, τ_0 , the initial wall shear stress, β_1 , the velocity factor of the wall shear stress when $n \neq 1$ and n , the wall velocity exponent. When m and n are 1, eqn (1) reduces to a four-paste parameter fit

$$P = 2(\sigma_0 + \alpha V) \ln \left(\frac{D_0}{D} \right) + 4(\tau_0 + \beta_1 V) \left(\frac{L}{D} \right) \quad (2)$$

where α and β replace α_1 and β_1 and have different units.

All paste formulations were characterised using the four-parameter model, eqn (2) and in addition the type II and III pastes were analysed using the six-parameter fit, eqn (1), by passing them through dies of 3 mm diameter, L/D ratios 1, 8 and 16 and at extrudate velocities of 0.001, 0.002, 0.005, 0.011, 0.021 and 0.053 m/s using a ram extruder with a barrel diameter of 25.4 mm. Pressure was recorded on the ram using a 20 kN load cell.

All the calculations were carried out by hand in this exercise, though computer programs were written for automated calculations. This dual approach was used because of the wish to evaluate the simplicity of the model and the degree of fit between models at all stages of the process.

In the Type I pastes a good agreement was obtained using the four-parameter characterisation. However, as shown in Fig. 1, using eqn (2) was inadequate for types II and III at intermediate extrudate velocities. In these materials the best fit was obtained using the six-parameter characterisation, eqn (1), which was resolved by extrapolating $P - L/D$ curves to zero L/D giving P_1 . The following equation can therefore be written

$$P_1/[2 \ln (D_0/D)] - \sigma_0 = \alpha_1 V^m \quad (3)$$

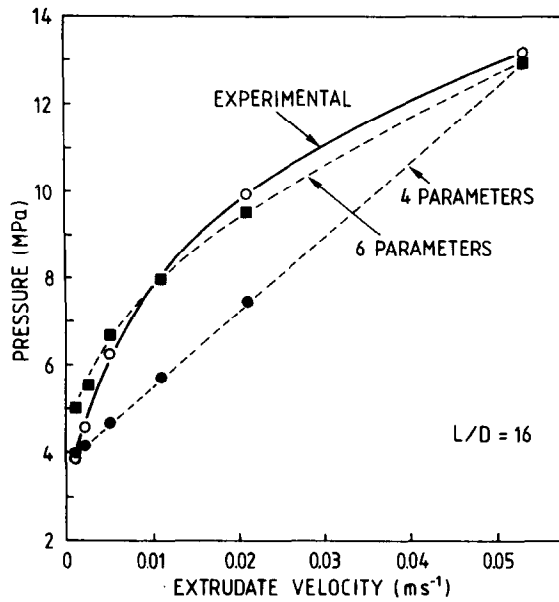


Fig. 1. Pressure-velocity relationships for a typical paste [II(8)].

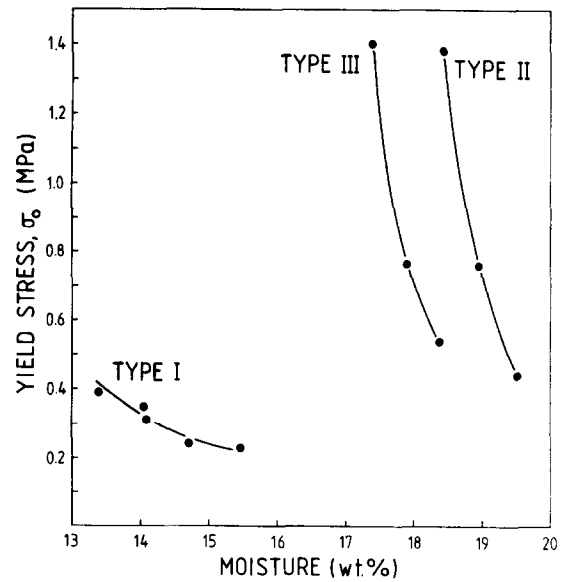


Fig. 2. Die entry yield stress plotted against moisture content.

which gives in ln-ln form, a straight line from which α_1 and m can be derived, σ_0 being derived from a plot of $P_1/2\ln(D_0/D)$ versus V . By subtracting P_1 from P to give P_2 a similar approach was used to resolve τ_0 , β_1 and n . Some difficulties were encountered in interpreting ln-ln plots derived from eqn (3) as straight lines were not produced in all cases. It is possible that eqns (1) and (2) require refinement to give better agreement of the data across the whole extrudate velocity range. The difficulties found in the fitting routine are reflected in the data, for example α_1 is high in paste II(7).

As expected the values of the parameters fall with increasing moisture content. Figure 2 shows

the relationship for σ_0 for the three paste types. The determined paste parameters are given in Table 2 for all the pastes examined.

Honeycomb Extrusion

All the pastes were passed through a model honeycomb die (Figs 3 and 4) at various extrudate velocities and, the required forces on the ram recorded. The results converted to pressure are given in Table 3. The pressure drop falls with increasing moisture in each paste type following similar trends to σ_0 in Fig. 2.

Table 2. Paste parameters

Paste no.	σ_0 (MPa)	α (MPa s m ⁻¹)	α_1 (MPa[s m ⁻¹] ^m)	m	τ_0 (MPa)	β (MPa s m ⁻¹)	β_1 (MPa[s m ⁻¹] ⁿ)	n
<i>Four-parameter fit</i>								
I(1)	0.39	0.49	—	—	0.034	0.59	—	—
I(2)	0.35	0.27	—	—	0.030	0.49	—	—
I(3)	0.31	0.45	—	—	0.025	0.47	—	—
I(4)	0.24	0.81	—	—	0.021	0.40	—	—
I(5)	0.23	0.00	—	—	0.017	0.34	—	—
II(6)	1.37	10.56	—	—	0.058	6.98	—	—
II(7)	0.80	6.74	—	—	0.053	3.77	—	—
II(8)	0.46	3.46	—	—	0.030	2.49	—	—
III(9)	1.41	12.58	—	—	0.048	7.68	—	—
III(10)	0.76	6.06	—	—	0.050	4.89	—	—
III(11)	0.56	4.04	—	—	0.038	4.43	—	—
<i>Six-parameter fit</i>								
II(6)	1.38	—	0.71	0.15	0.057	—	2.18	0.60
II(7)	0.76	—	2.39	0.60	0.053	—	1.08	0.57
II(8)	0.44	—	0.74	0.50	0.031	—	0.59	0.51
III(9)	1.40	—	1.31	0.35	0.048	—	1.48	0.43
III(10)	0.76	—	0.76	0.48	0.050	—	1.25	0.50
III(11)	0.54	—	0.57	0.43	0.039	—	0.67	0.44

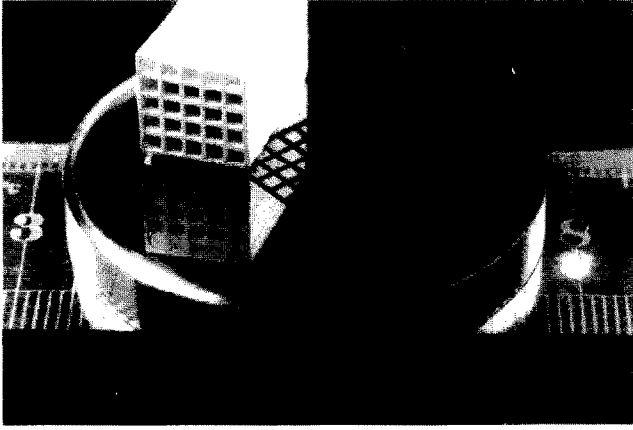


Fig. 3. The experimental honeycomb die and an extrudate produced from it.

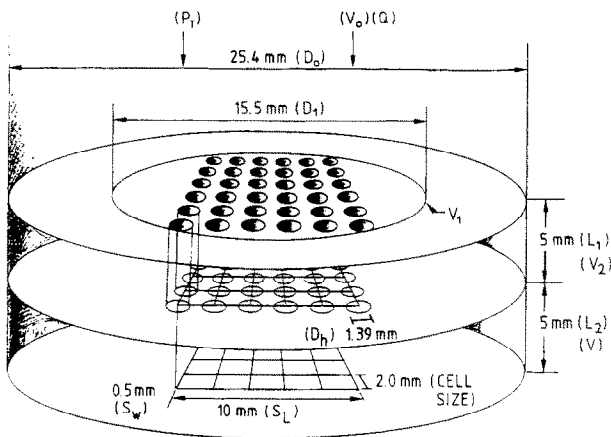


Fig. 4. Schematic cross-section of experimental honeycomb die, P_T is the total pressure drop through the die, V_0 is the ram velocity, Q is the volumetric flow rate, D_1 is the diameter of a circle which just touches the outermost holes of the back plate, V_1 is the velocity of the extrudate as it passes D_1 , D_h is the die hole diameter, L_1 is the length of the die holes, V_2 is the velocity of the paste in the die holes, L_2 is the length of the slots, S_w is the width of the slots, S_L is the side length of the extrudate, V is the velocity of the extrudate in the slots and at the exit of the die.

Model Development

It should be possible by developing geometrically corrected equations based on eqns (1) and (2) to predict the pressure drop through the die based on the paste parameters given in Table 2. The die can be broken down into four regions: the entry into the multi-holes, flow in the multi-holes, the transition from holes to slots and flow in the slots. The dimensions of the die and the notation for the various components are given in Fig. 4. Flow into the multi-holes from the barrel can be modelled in a single equation, P_A , (the derivation of which is given by Benbow *et al.*,⁴ and Benbow and Bridgwater²) or can be split into two components where the flow into a large die of diameter equal to D_1 is first calculated, related to P_1 in eqn (1) followed

Table 3. Experimental honeycomb pressure drops (MPa)

Paste no.	Extrudate velocity			
	0.0016 m/s	0.0078 m/s	0.014 m/s	0.021 m/s
I(1)	2.29	2.49	2.62	2.68
I(2)	1.87	1.99	2.01	2.11
I(3)	1.60	1.74	1.78	1.84
I(4)	1.40	1.56	1.66	1.74
I(5)	1.18	1.24	1.34	1.40
II(6)	11.74	14.47	15.59	16.70
II(7)	6.04	7.66	8.64	9.20
II(8)	3.20	4.16	4.80	5.05
III(9)	9.89	12.57	13.52	14.60
III(10)	5.60	7.36	8.19	9.04
III(11)	3.77	4.97	5.59	5.92

by the flow into the multi-hole plate, P_B . The equations for these two alternatives are

$$P_A = 2 \left[\sigma_0 + \frac{\alpha 4Q}{\pi D_h^2 N} \right] \ln \left(\frac{D_0}{D_h \sqrt{N}} \right) \quad (\text{four parameters}) \quad (4a)$$

$$P_A = 2 \left[\sigma_0 + \alpha_1 \left(\frac{4Q}{\pi D_h^2 N} \right)^m \right] \ln \left(\frac{D_0}{D_h \sqrt{N}} \right) \quad (\text{six parameters}) \quad (4b)$$

$$P_B = 2(\sigma_0 + \alpha V_1) \ln \left(\frac{D_0}{D_1} \right) + 2 \left[\sigma_0 + \frac{\alpha 4Q}{\pi D_h^2 N} \right] \ln \left(\frac{D_1}{D_h \sqrt{N}} \right) \quad (\text{four parameters}) \quad (5a)$$

$$P_B = 2(\sigma_0 + \alpha_1 V_1^m) \ln \left(\frac{D_0}{D_1} \right) + 2 \left[\sigma_0 + \alpha_1 \left(\frac{4Q}{\pi D_h^2 N} \right)^m \right] \ln \left(\frac{D_1}{D_h \sqrt{N}} \right) \quad (\text{six parameters}) \quad (5b)$$

where N is the number of die holes. The flow in the multiple holes⁴ is given by

$$P_C = 4 \left[\tau_0 + \frac{\beta 4Q}{\pi D_h^2 N} \right] \left(\frac{L_1}{D_h} \right) \quad (\text{four parameters}) \quad (6a)$$

$$P_C = 4 \left[\tau_0 + \beta_1 \left(\frac{4Q}{\pi D_h^2 N} \right)^r \right] \left(\frac{L_1}{D_h} \right) \quad (\text{six parameters}) \quad (6b)$$

The pressure drop between hole and slot can be calculated in two alternative ways. The change in total open area from holes to slots can be used to develop an equation, P_D , or the change in area from the holes to the area of slot exposed down the holes can be used to give an alternative equation, P_E ,⁴ Fig. 5. These two possibilities are resolved by the following equations

$$P_D = (\sigma_0 + \alpha V) \ln \left(\frac{A_h}{A_s} \right) \quad (\text{four parameters}) \quad (7a)$$

$$P_D = (\sigma_0 + \alpha_1 V^m) \ln \left(\frac{A_h}{A_s} \right) \quad (\text{six parameters}) \quad (7b)$$

$$P_E = (\sigma_0 + \alpha V) \ln \left(\frac{A_h}{[2\{D_h - S_w\} S_w + S_w^2][\sqrt{N} - 2]^2 + [1.5\{D_h - S_w\} S_w + S_w^2][\sqrt{N} - 2]4 + [\{D_h - S_w\} S_w + S_w^2]4} \right) \quad (\text{four parameters}) \quad (8a)$$

$$P_E = (\sigma_0 + \alpha_1 V^m) \ln \left(\frac{A_h}{[2\{D_h - S_w\} S_w + S_w^2][\sqrt{N} - 2]^2 + [1.5\{D_h - S_w\} S_w + S_w^2][\sqrt{N} - 2]4 + [\{D_h - S_w\} S_w + S_w^2]4} \right) \quad (\text{six parameters}) \quad (8b)$$

where A_h and A_s are the open areas of the holes and slots respectively. The final contribution to pressure drop is the flow through the slots, P_F , which is given by

$$P_F = 4(\tau_0 + \beta V) \left(\frac{ML_2}{A_s} \right) \quad (\text{four parameters}) \quad (9a)$$

$$P_F = 4(\tau_0 + \beta_1 V^m) \left(\frac{ML_2}{A_s} \right) \quad (\text{six parameters}) \quad (9b)$$

where M is the perimeter length of the slots. Four models are thus constructed here by combining eqns (4)–(9) as follows:

$$1a = P_A + P_C + P_D + P_F,$$

$$1b = P_B + P_C + P_D + P_F,$$

$$2a = P_A + P_C + P_E + P_F,$$

$$2b = P_B + P_C + P_E + P_F.$$

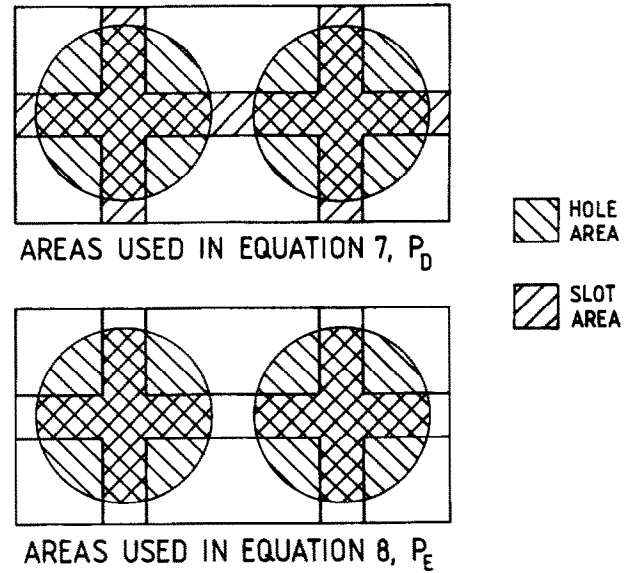


Fig. 5. Schematic representation of the areas used in the calculation of the pressure drop in the holes-to-slots transition.

Results and Discussion of the Honeycomb Model Fit

All the predicted values for the pastes examined are given in Table 4 as a percentage of the experimental values given in Table 3. Figure 6 shows the fit of the four models (1a, 1b, 2a and 2b) to the experimental data points for pastes I(2) and II(8), using paste parameters derived by four- and six-parameter characterisation, respectively. It can be seen that in both cases models of form 2, incorporating eqn (8) agree with the experimental points most closely. It is to be expected that models of form 1, incorporating eqn (7) will yield lower values because, if the holes and the slots had the same open area the predicted pressure drop would be zero. This is improbable as some resistance must occur in the transition from holes to slots. The differences between the a and b models, i.e. between P_A and P_B are small in the Type I pastes showing that the models are largely interchangeable. In the Type II and III pastes eqn (4) tends to give greater pressure drops than eqn (5). This can be attributed to some deficiency in the models when the materials show a strong velocity dependence.

It is clear from Figs 6 and 7 that pastes of Type I are generally modelled well by the eqns (4)–(9) across the whole range of the experimental velocities, ranging between +10% and –10% of the experimental value for model 2a. For this same model in Type II and III pastes the predicted values are consistently low, typically between –10 and –45%.

The figures in Table 4 show that, in the Type II and Type III pastes, better estimates of the

Table 4. Predicted pressure drops as a percentage of the experimental values presented in Table 3

Model	1a			1b			2a			2b						
	0.0014	0.0078	0.014	0.021	0.0014	0.0078	0.014	0.021	0.0014	0.0078	0.014	0.021				
<i>Extrudate velocity (m/s)</i>																
<i>Four-paste parameter data</i>																
I(1)	86.56	84.67	84.94	88.26	86.54	84.57	84.76	87.99	93.52	91.13	91.10	94.33	93.49	91.02	90.92	94.07
I(2)	94.51	93.97	98.06	98.86	94.50	93.89	97.93	98.67	102.25	101.28	105.34	105.83	102.23	101.20	105.21	105.65
I(3)	94.53	92.74	96.28	99.27	94.50	92.60	96.03	98.92	102.45	100.10	103.54	106.37	102.42	99.96	103.30	106.02
I(4)	88.65	85.49	85.86	87.83	88.59	85.21	85.39	87.15	95.89	92.12	92.23	94.04	95.83	91.84	91.75	93.36
I(5)	94.03	94.88	92.84	94.24	94.04	94.92	92.91	94.33	102.12	102.57	99.95	101.03	102.13	102.61	100.01	101.12
II(6)	45.15	47.23	53.65	60.41	45.05	46.84	52.99	59.49	50.00	51.36	57.65	64.34	49.91	50.97	57.00	63.42
II(7)	61.19	59.24	62.21	68.77	61.07	58.77	61.46	67.70	66.71	63.83	66.48	72.99	66.59	63.35	65.72	71.92
II(8)	66.44	64.02	66.90	75.57	66.32	63.58	66.20	74.57	72.43	68.84	71.26	79.91	72.31	68.39	70.56	78.92
III(9)	51.62	54.11	62.88	71.29	51.48	53.57	61.98	70.04	57.55	59.03	67.70	76.00	57.42	58.49	66.79	74.74
III(10)	63.65	62.78	69.30	75.92	63.53	62.34	68.59	74.95	69.31	67.31	73.56	79.97	69.20	66.87	72.85	79.00
III(11)	70.36	68.14	73.87	83.68	70.25	67.70	73.17	82.69	76.55	73.04	78.41	88.16	76.43	72.60	77.71	87.17
<i>Six-paste parameter data</i>																
II(6)	52.57	52.18	54.37	56.02	50.50	49.85	52.01	53.68	58.53	57.08	59.00	60.40	53.46	51.88	53.77	55.25
II(7)	64.80	61.92	61.50	63.69	64.01	60.30	59.48	61.29	70.33	66.71	66.01	68.16	68.62	63.33	61.88	63.33
II(8)	73.84	68.94	66.75	69.31	73.18	67.88	65.55	67.94	79.88	73.93	71.28	73.77	77.91	70.68	67.57	69.54
III(9)	63.74	62.94	65.52	66.28	62.39	61.07	63.40	64.01	70.14	68.31	70.68	71.19	67.12	64.21	66.07	66.33
III(10)	73.10	69.62	70.64	70.64	72.50	68.65	69.48	69.37	78.93	74.29	74.96	74.64	77.61	72.19	72.51	72.00
III(11)	81.96	75.88	74.93	76.78	81.14	74.69	73.59	75.31	88.20	80.90	79.55	81.25	86.17	77.91	76.18	77.54

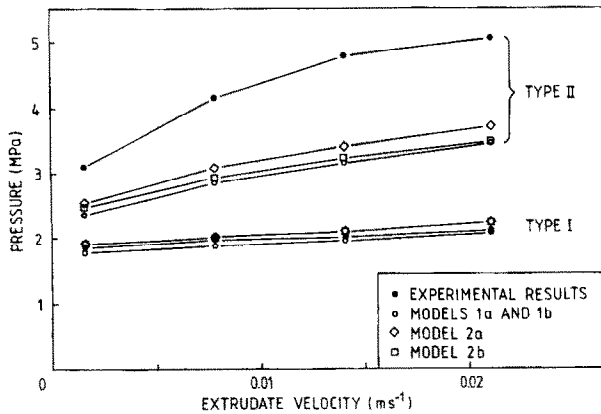


Fig. 6. Pressure drop in honeycomb extrusion, predicted and experimental for pastes I(2) and II(8).

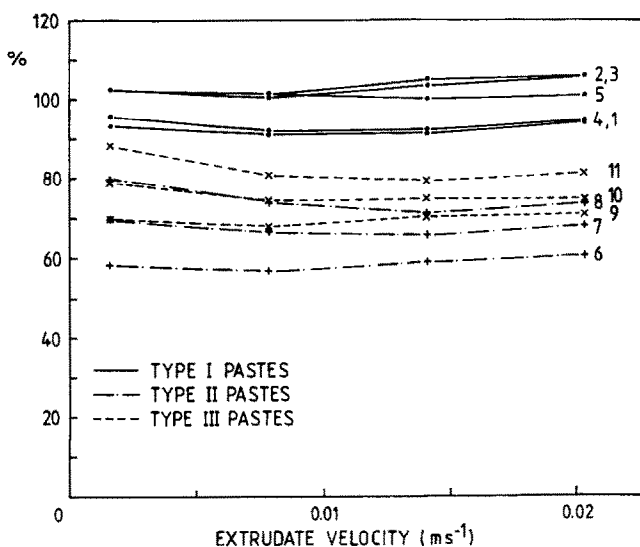


Fig. 7. Predicted pressure drop as a percentage of the experimental value at different extrudate velocities.

experimental pressure drops were obtained particularly at low velocities, by using the six-parameter equations. The differences in fit between the various paste types can only be attributable to the differences in the rheology of the pastes as the honeycomb models are consistent in all cases. In pastes of Type I, α is generally small and there is a linear relationship between P and V for a given L/D . It would appear that under these circumstances the shortcomings of the honeycomb models presented are masked. Where the pastes show a marked and non-linear dependence on velocity in both convergent and laminar flow the model does not correlate exactly with the experimentally observed pressure drop. It appears that the major contributing factor to this underestimation is the spreading which must occur after the transfer from the holes to the slots before the streams fully

unite, giving the honeycomb structure. This divergent flow requires work to be done, but as yet the models describing such flow in terms of the paste flow parameters used here are only now being developed.^{5,6} A further alternative solution could be to use a 'universal' approach⁷ based on the model concept. However, in this system the relationships for multi-hole and complex geometry have not been evaluated. Thus the present models are only applicable for specific rheologies if accurate pressure drop predictions are required. However, the models may be applicable to other pastes in their current form if the errors are considered systematic for that particular paste system.

Conclusion

Paste flow in honeycomb dies can be modelled with reasonable accuracy for some paste types where the flow is simple and the velocity dependence in convergent flow is small. The flow of more complex pastes is less predictable and this is attributed to a paste divergent term at the hole to slot transition.

Acknowledgements

The authors wish to thank the EPSRC for their support and Dr J. Benbow for his help and encouragement in preparing this work.

References

1. Benbow, J. J., Ford, L. W. & Heath, D. J., Support and Catalyst. *British Patent No. 138590M*, 1972.
2. Benbow, J. J. & Bridgwater, J., *Paste flow and extrusion. Oxford Series on Advanced Manufacturing Vol. 10*, Clarendon Press, Oxford, 1993.
3. Benbow, J. J., Oxley, E. W. & Bridgwater, J., The extrusion mechanics of pastes — the influence of paste formulation on extrusion parameters. *Chem. Eng. Sci.*, **42** (1987) 2151.
4. Benbow, J. J., Jazayeri, S. H. & Bridgwater, J., The flow of pastes through dies of complicated geometry. *Powder Technol.*, **65** (1991) 393–401.
5. Bates, A. J. D. & Bridgwater, J., The flow of pastes in complex geometries. *ICHEME Res. Event Procs.*, **1** (1993) 378–380.
6. Bates, A. J. D. & Bridgwater, J., Modelling of non-uniform radial flow. *ICHEME Res. Event Procs.*, **2** (1994) 725–727.
7. Benbow, J. J., Lawson, T. A., Oxley, E. W. & Bridgwater, J., Prediction of paste extrusion pressure. *Ceram. Bull., Amer. Ceram. Soc.*, **68** (1989) 1821–1824.